0021-8928(94)00074-3

A THERMALLY NON-EQUILIBRIUM VISCOUS SHOCK LAYER PAST SLENDER BLUNTED CONES†

S. V. ZHLUKTOV, G. A. TIRSKII and S. V. UTYUZHNIKOV

Moscow

Physical–chemical processes in a shock layer past a slender spherically blunted body at high supersonic velocities are investigated. Using a gas-dynamic model, defined by the complete viscous shock-layer equations [1], the steady laminar axisymmetric flow of viscous, heat-conducting, partially dissociated and ionized air under chemical and thermal non-equilibrium is considered throughout the region between the body and the required thin shock wave. Attention is concentrated on the non-equilibrium chemical, ionization, and relaxation kinetics at large distances from the leading stagnation point. Multicomponent diffusion and the reverse influence of dissociation–recombination on the relaxation of vibrational quantum states, i.e. coupling vibration–dissociation–vibration (CVDV), are taken into account. A new model is used to describe dissociation–relaxation process [2]. The model includes the effect of non-equilibrium excitation of vibrations and the equilibrium excitation of rotational molecular modes on the dissociation rate constants. Comparisons with experimentally verified calculations and calculations within the scope of the chemically equilibrium full viscous shock-layer model indicate that the model is physically adequate. The calculations highlighted physical effects in the non-equilibrium viscous shock layer past a slender spherically blunted cone at various distances from the stagnation point.

The above effects and their influence on the heat transfer to the body and drag have been studied in detail in [3, 4] in the stagnation region. However, the use of the CVDV model [4] introduces an uncertainty due to the indefiniteness in the probability of dissociation from various molecular vibrational levels at high temperatures $T \geqslant 8000$ K the probability being expressed in exponential form with a single empirical parameter (the phenomenological approach [5]). To overcome the uncertainty in the dissociation model, an approach [2] was suggested based on a quantum consideration of dissociation. The model from [2] is employed in the present study. To integrate the system of axisymmetric viscous shock-layer equations, a block-marching method of global iterations is used [6].

1. THE GOVERNING EQUATIONS AND BOUNDARY CONDITIONS

Consider hypersonic flows of viscous, heat-conducting, chemically reacting nine-component air O_2, N_2, NO, O, N, NO^+, N_2^+, N^+, E (electron) past spherically blunted slender cones of 150–200 nose radii. It is assumed that the active (translational and rotational) quantum states of the particles of the mixture are in equilibrium with one another at the translational temperature T, and the vibrational quantum states of the ith molecules have a Boltzmann distribution at a certain vibrational temperature $T_i^{(V)}$. In the general case $T_i^{(V)} \neq T$. The contribution of

excited electron quantum states to the internal energy of the mixture is ignored. It is assumed that all the particles of the mixture are in ground electron states and ionization starts from these states.

The effects of pressure diffusion and thermal diffusion are ignored. Pressure diffusion has a greater influence on the flow because the pressure diffusion factors are larger by an order of magnitude than those for thermal diffusion. The pressure diffusion effect consists of a re-distribution of the species fractions and diffusive fluxes in the neighbourhood of the shock wave [7] where maximum pressure gradients and other hydrodynamic quantities occur. Pressure diffusion has almost no effect on the velocity, pressure, density and temperature in the shock layer. Pressure diffusion reduces the heat flux to the body by no more than 2%, and the equilibrium temperature of the surface by no more than 10°.

Chemical reactions in the shock-wave region can also be ignored [7], because their influence on the heat flux to the body is limited to 1%. Hence, the flow in the shock layer can be considered separately from the flow in the shock wave. Radiation has little effect on the structure of the flow in the regimes under consideration, and is therefore also ignored.

The complete system of two-dimensional (axisymmetric) viscous shock layer (VSL) equations for chemically non-equilibrium (thermally equilibrium) flows is given in [1] in an orthogonal system of coordinates (x, y) normally connected with the body, where x is the distance along the surface of the body from the stagnation point, and y is the distance along the normal from the surface of the body to the given point in the flow. Here we will only give the expression for the normal component of the energy flux J_{Hy} for a mixture of gases under chemical non-equilibrium and thermal equilibrium, which will be required below

$$J_{Hy} = -\frac{\lambda}{C_p}\left[\frac{\partial H}{\partial y} - \upsilon_1 \frac{\partial \upsilon_1}{\partial y} - \upsilon_2 \frac{\partial \upsilon_2}{\partial y} - \sum_{i=1}^{N} h_i \frac{\partial c_i}{\partial y}\right] - \upsilon_1 \tau_{xy} + \sum_{i=1}^{N} h_i J_{iy} \tag{1.1}$$

where λ and C_p are the thermal conductivity and heat capacity of the mixture, H is the total enthalpy of the mixture, υ_1 and υ_2 are the streamwise and normal components of the velocity, h_i are the specific enthalpies, N is the total number of species, J_{iy} and c_i are the normal components of the diffusive fluxes and mass fractions of species, and τ_{xy} is the mixed component of the viscous stress tensor.

In the case of thermal non-equilibrium (i.e. when there is no equilibrium between different modes of the particles of the mixture), the system of chemically non-equilibrium VSL equations must be supplemented by equations describing the energy exchange between different quantum states of the species. If the rotational modes of the molecules are in equilibrium with the translational ones, the vibrational quantum states of the ith molecules have a Boltzmann distribution at some vibrational temperature $T_i^{(V)} \neq T$, and all the particles of the mixture are in ground electron states, as in our case, then one must add the equations for vibrational energies of the molecular components [8] to the original system

$$\rho\left[\frac{\upsilon_1}{H_1}\frac{\partial}{\partial x}(\varepsilon_i c_i) + \upsilon_2 \frac{\partial}{\partial y}(\varepsilon_i c_i)\right] + \frac{1}{H_1 r^\nu}\frac{\partial}{\partial y}\left[H_1 r^\nu\left(\varepsilon_i J_{iy} - \mu\frac{c_i}{S_i}\frac{\partial \varepsilon_i}{\partial y}\right)\right] = W_i^{(V)}$$

$$H_1 = 1 + \frac{y}{R}, \quad r = r_w + y\cos\alpha, \quad S_i = \sum_{j=1}^{N} S_{ij} x_i \tag{1.2}$$

Here ρ is the density, H_1 and r are Lamé coefficients, $R(x)$ is the local radius of curvature of the body, $r_w(x)$ is the distance from the body surface to the axis of symmetry, $r(x, y)$ is the distance between a point in the flow and the axis of symmetry, α is the angle between the tangent to the body and the axis of symmetry, $\nu = 0$ for plane flow and $\nu = 1$ for axisymmetric flow, S_{ij} are the binary Schmidt numbers, x_j are molar fractions of species, and $\varepsilon_i(T_i^{(V)})$ is the average vibrational energy of the ith molecular species, which is calculated using the model of an harmonic oscillator truncated at the dissociation energy kT_{Di} (k is Boltzmann's constant)

$$\varepsilon_i = R_A \left[\frac{\theta_i}{\exp(\theta_i / T_i^{(V)}) - 1} - \frac{T_{Di}}{\exp(T_{Di} / T_i^{(V)}) - 1} \right] \tag{1.3}$$

where θ_i is the characteristic vibrational temperature of the ith molecular species, and $W_i^{(V)}$ is the source term for the vibrational energy, which accounts for the energy exchange between the vibrational quantum states of the ith molecular species and the other modes of the particles of the mixture. In the general case $W_i^{(V)}$ includes the rate of energy exchange with active modes (V–T exchange), with vibrational modes of the other molecular species (V–V′ exchange), with translational modes of free electrons (E–V exchange), and the loss (gain) of vibrational energy in dissociation (recombination). We will neglect the terms due to V–V′ and E–V processes because of their relative smallness for the present range of free-stream conditions. Hence, two terms remain in the expression for $W_i^{(V)}$

$$W_i^{(V)} = c_i \frac{\varepsilon_i(T) - \varepsilon_i(T_i^{(V)})}{\tau_i} - W_{Di} \tag{1.4}$$

The following expression is used for the vibrational relaxation time

$$\tau_i = \{P_{atm} \Sigma_r x_r \exp[18.42 - 1.16 \times 10^{-3} \mu_{ir}^{\frac{1}{2}} \theta_i^{\frac{4}{3}} (T^{-\frac{1}{3}} - 0.015 \mu_{ir}^{\frac{1}{4}})]\}^{-1} + \{P \sigma_v \langle V_i \rangle n\}^{-1},$$

$$\mu_{ir} = m_i m_r / (m_i + m_r) \tag{1.5}$$

where P_{atm} is the pressure measured in atmospheres, $\langle V_i \rangle$ is the average thermal velocity of the ith species, σ_v is the average cross-section for the excitation of vibrations, and n is the total concentration of the particles of the mixture. Summation is performed only over the heavy species. The first term in the expression for the vibrational relaxation time is the well-known formula [9]. The term $\{\sigma_v \langle V_i \rangle n\}^{-1}$ enables more realistic values to be obtained for τ_i when $T \geqslant 10^4$ K [10]. We use the following expression for σ_v [11]

$$\sigma_v = 10^{-9} (5/T)^2 \text{ cm}^2 \tag{1.6}$$

The influence of chemical reactions on the vibrational relaxation is taken into account by the source term

$$W_{Di} = \rho^2 m_i \left[K_{Di}(T, T_i^{(V)}) \frac{c_i}{m_i} \varepsilon_i(T_m) - \rho K_{Ri}(T) \frac{c_{A1}}{m_{A1}} \frac{c_{A2}}{m_{m2}} \frac{R_A T_{Di}}{2} \right] \tag{1.7}$$

$$T_m^{-1} = (T_i^{(V)})^{-1} - T^{-1} \tag{1.8}$$

Here A_1 and A_2 are the atoms of the ith molecular species, K_{Di} and K_{Ri} are the dissociation and recombination rate constants, and $\varepsilon_i(T_m)$ and $R_A T_{Di}/2$ are the average values of the energy lost and gained by vibrations in dissociation and recombination, respectively.

Summing Eqs (1.2) over the molecules and assuming that all the molecules have a Boltzmann distribution over the vibrational levels at some average vibrational temperature $T^{(V)}$, which is valid for air molecules, one can obtain an equation for the average vibrational temperature $T^{(V)}$ [3].

It should be noted that under the condition of thermal non-equilibrium, expression (1.1) for the energy flux somewhat change its form: it is necessary to replace λ, C_p and Pr by λ^{act}, C_p^{act} and Pr^{act} (the thermal conductivity, heat capacity and Prandtl number due to active, i.e. translational and rotational, degrees of freedom), and add to the right-hand side the quantity

$$\frac{\partial T^{(V)}}{\partial y} \frac{\lambda^{act}}{C_p^{act}} \sum_{j=M} \varepsilon_j' \frac{c_j}{m_j} \left(1 - \frac{Pr^{act}}{S_j} \right) \tag{1.9}$$

The prime denotes differentiation of the vibrational energy ε_i (see (1.3)) with respect to the vibrational temperature $T^{(V)}$; we also have

$$h_A = h_A^0 + 2.5 \cdot R_A T / m_A, \quad h_M = h_M^0 + (3.5 \cdot R_A T + \varepsilon_M(T^{(V)}))/ m_M \tag{1.10}$$

where h_A^0 and h_M^0 are the enthalpies of formation of the atoms and molecules.

The effect of thermal non-equilibrium $(T^{(V)} \neq T)$ on the dissociation rates is taken into account by using an expression approximating the two-temperature dissociation rate constant [2] for the ith molecule undergoing collision with the jth particle of the mixture

$$K_{D_{ij}} = \sqrt{\frac{8 R_A T}{\pi \mu_{ij}}} \sigma_{ij} \frac{1}{Z_i(T^{(V)})} \frac{1}{(kT)^2} \exp\left[-\frac{T_{Di}}{T} \right] \Phi_{ij}$$

$$\Phi_{ij} = \frac{1}{2} kT_{Di}\gamma_i (kT_{Di}\gamma_i + 2kT) \exp(-\beta_{ij}\sqrt{kT_{Di}\gamma_i})Z_i(T_m) \tag{1.11}$$

$$\gamma_i = 1 - 0.8 \frac{\varepsilon_i(T_m)}{R_A T_{Di}}, \quad \beta_{ij} = \frac{1}{h\alpha_{ij}}\sqrt{\frac{\mu_{ij}}{2 N_A}}$$

$$Z_i(T^{(V)}) = [1 - \exp(-T_{Di} / T^{(V)})] / [1 - \exp(-\theta_i / T^{(V)})]$$

Here Z_i is the vibrational partition function for the ith truncated oscillator, σ_{ij} is the gas-kinetic cross-section for collisions of the ith molecule with the jth species, N_A is Avogadro's number, and α_{ij} (Å^{-1}) is a parameter determining the long-acting potential of interaction between the ith and jth species of the mixture

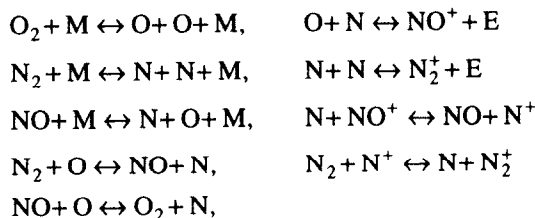$$V_{ij} = V_{ij}^0 \exp(-\alpha_{ij} r) \tag{1.12}$$

where r (Å) is the distance between the interacting particles.

We assume that only the molecular dissociation rate constants depend on the two temperatures T and $T^{(V)}$. All the other reactions (recombination, ionization, exchange, and charge-transfer) depend only on the temperature T of the active degrees of freedom. For the recombination rate constants we use the expression

$$K_{R_{ij}} = K_{D_{ij}}(T, T)/K_{C_i}(T) \tag{1.13}$$

where $K_{D_{ij}}$ is calculating using formulae (1.11). Data from [13] are used for the equilibrium constants K_{C_i}, exchange, ionization and charge-transfer rate constants.

The following system of chemical reactions is considered

$$O_2 + M \leftrightarrow O + O + M, \qquad O + N \leftrightarrow NO^+ + E$$

$$N_2 + M \leftrightarrow N + N + M, \qquad N + N \leftrightarrow N_2^+ + E$$

$$NO + M \leftrightarrow N + O + M, \qquad N + NO^+ \leftrightarrow NO + N^+$$

$$N_2 + O \leftrightarrow NO + N, \qquad N_2 + N^+ \leftrightarrow N + N_2^+$$

$$NO + O \leftrightarrow O_2 + N,$$

To compute the viscosity and "transport" thermal conductivity, the latter being solely due to translational degrees of freedom, we use the approximation formulae [14], which enable these coefficients to be obtained with a high degree of accuracy over a wide range of temperatures and pressures. In order to take into account the contribution of rotational modes (and vibrational ones in the case of thermal equilibrium) to the thermal conductivity of the mixture, the Eaken correction [15] is used.

Generalized Rankine–Hugoniot relations [1] are used at the shock wave. The appropriate condition for Eq. (1.2) has the form [3]

$$c_i \varepsilon_i |_\infty = c_i \varepsilon_i |_s - \frac{\cos \beta_s}{\rho_\infty V_\infty \sin \beta} \left(\varepsilon_i J_{iy} - \mu \frac{c_i}{S_i} \frac{\partial \varepsilon_i}{\partial y} \right) \Big|_s, \quad \beta_s = \beta - \alpha \tag{1.14}$$

The subscripts ∞ and s correspond to the parameter values directly in front of and behind the shock wave, and β and α are the angles of inclination of the tangents to the shock wave and to the body surface, respectively. Flow regimes are considered for which the shock wave is fairly thin. Hence we can neglect the energy exchange between vibrational and active modes in the few collisions that occur in the shock-wave region.

The no-slip and no-flow conditions are used, respectively, for the tangential and normal projections of the momentum equation on the body surface (the former condition being valid for a relatively cold wall at high Reynolds numbers). Heat balance is assumed for the energy equation on the surface

$$J_{Hy}|_w = J_{qy}|_w = -\hat{\sigma}\hat{\varepsilon}T_w^4 \tag{1.15}$$

The subscript w corresponds to the parameter values on the body surface, J_{qy} is the normal component of the heat flux, $\hat{\sigma} = 5.67 \times 10^{-8}$ W/m^2 K^4 (or kg/s^3 K^4) is the Stefan–Boltzmann constant, $\hat{\varepsilon} = 0.8$ is the blackness of the body surface.

The surface conditions for the equations of conservation of mass of the reaction products can be written as follows:

$$J_{iy}|_w = -k_w \rho c_i |_w \tag{1.16}$$

where k_w is the effective catalytic activity of the surface. The limiting cases of non-catalytic ($k_w = 0$) and fully catalytic ($k_w = \infty$, i.e. $c_i|_w = 0$) surfaces are considered for neutral reaction products, while the surface is assumed to be fully catalytic for charged species. The boundary conditions for the remaining species follow from the condition of zeroth mass fluxes of elements to the non-disintegrating wall.

For the equation of vibrational relaxation the following boundary condition is used [16]

$$\partial T^{(V)}/\partial y|_w = 0 \tag{1.17}$$

This condition expresses the fact that there is no vibrational energy flux

$$J_{qy}^{(V)} = \sum_{j=M} \frac{\varepsilon_j(T^{(V)})}{m_j} J_{jy} - \frac{\partial T^{(V)}}{\partial y} \mu \sum_{j=M} \varepsilon_j' \frac{c_j}{m_j S_j} \tag{1.18}$$

to a non-catalytic body surface (μ is the dynamic viscosity). The case of a thermally non-equilibrium flow near a fully catalytic surface is not considered, because the flow is less sensitive to thermal non-equilibrium. Note that expression (1.18) follows directly from the classical expression for the heat flux in terms of the temperature gradient and diffusive fluxes under the assumption of non-equilibrium thermodynamics

$$\mathbf{J}_q = -\lambda^{act} \nabla T + \sum_{j=1}^{N} h_j \mathbf{J}_j - \mu \sum_{j=M} \nabla \varepsilon_j \frac{c_j}{m_j S_j} \tag{1.19}$$

2. NUMERICAL METHOD

It is known that the full set of VSL equations has elliptic properties. To solve the system we use the global iteration (GI) method. To compute correctly the flow properties at the point of the sphere and cone conjugation, the exact relations have previously been obtained [6] on the line of discontinuity of the first and second derivatives.

To integrate the original system of equations, we employ an implicit finite-difference scheme of the second order of approximation along the body, and of the fourth order of approximation across the layer. About 8 GIs are necessary for the solution to converge over the blunted part of the body, and 2–3 GIs are necessary for every computational block over the cone. At each step along the marching coordinate the full non-linear system of multicomponent non-equilibrium VSL equations is solved by Newton's method. Note that the use of a difference scheme of the fourth order of approximation along the normal coordinate, in combination with an adaptive grid which is recondensed along the body, allows the calculations to be performed at high Reynolds numbers $Re_\infty = \rho_\infty V_\infty R(0)/\mu_\infty$ (of the order of 10^6–10^8), and the flow at $Re_\infty = 10^8$ requires 20% more computer time than flow at $Re_\infty = 10^6$ [17]. Note also that the algorithm for solving the complete VSL system does not require any parameter smoothing in the streamwise and normal directions.

3. NUMERICAL RESULTS

The purpose of this investigation is to test the algorithm for integrating the complete system of VSL equations and to study the main physical–chemical effects which occur in a shock layer at large distances from the stagnation point.

Calculations of the heat flux to the surface of the body at the stagnation point, performed within the scope of the multicomponent non-equilibrium full VSL model, have been shown to be in a good agreement with data [18] obtained within the framework of a thin-VSL model for clean nitrogen, which, in turn, are in a good agreement with experiment for the flow of dissociating nitrogen around a spherically blunted body.

Two flow regimes were chosen for comparison: (1) $\rho_\infty = 2.33 \times 10^{-4}$ kg/m^3 and $R_0 = 0.33$ m (where R_0 is the radius of the sphere), and (2) $\rho_\infty = 6.99 \times 10^{-4}$ kg/m^3 and $R_0 = 0.95$ m at a fixed free-stream velocity $V_\infty = 6490$ m/s and a fixed temperature of the body surface $T_w = 1500$ K.

For the first regime the difference between the heat flux values calculated within the two codes is 6% when $k_w = 0$ and 5% when $k_w = \infty$ and for the second regime it is 12% when $k_w = 0$ and 3% when $k_w = 0$.

To compare the values of the relative heat flux $q^{rel} = J_{q_w}|_{k_w=0} / J_{q_w}|_{k_w=\infty}$ with the data [19], the flow around a spherically blunted cone with a half-angle of $10°$ and the nose radius $R_0 = 0.2286$ m at a velocity $V_\infty = 8170$ m/s, height 53.34 km ($Re_\infty = 76810$, $M_\infty = 25$) and fixed surface temperature $T_w = 1256$ K was chosen.

In Fig. 1, curve 1 (the dashed line) is the result given in [19], solid curve 2 is obtained using the thermally equilibrium chemically non-equilibrium complete VSL model with fixed surface temperature $T_w = 1256$ K assuming binary diffusion and Le = const = 1.4. The abscissa is the distance along the body surface relative to the nose radius: $x' = x/R_0$. It is clear that the difference in the values of q^{rel} between the data of [19] and the data obtained by the non-equilibrium complete VSL model is negligible on the sphere, reaches 23% immediately behind the conjugation point, and decreases gradually along the cone. The discrepancy may be due to the smoothing used in [19].

The quantity q^{rel} obviously cannot reflect all the physical effects occurring in the hypersonic shock layer. Therefore we will also present some other flow characteristics corresponding to the above-specified flow (a cone of half-angle $10°$, $R_0 = 0.2286$ m, $V_\infty = 8170$ m/s, and height 53.34 km) over the radiationally equilibrium surface (boundary condition (1.15)).
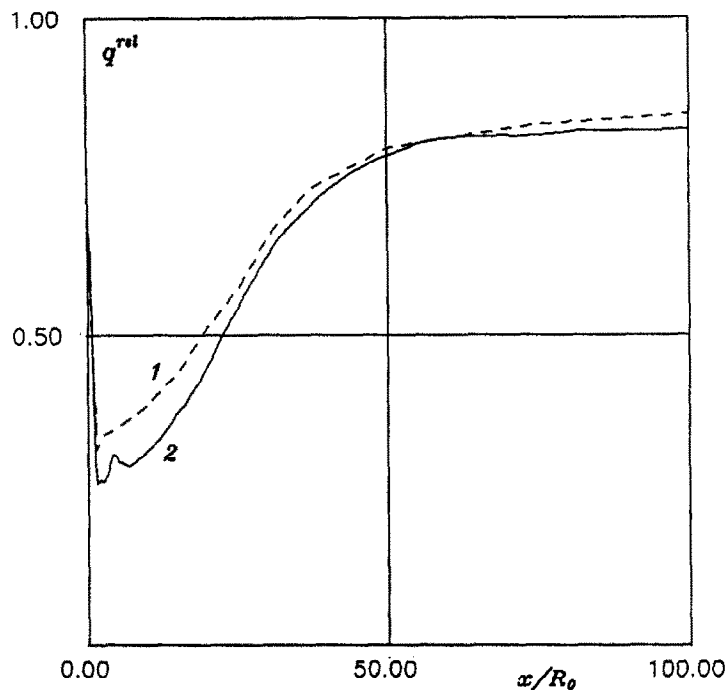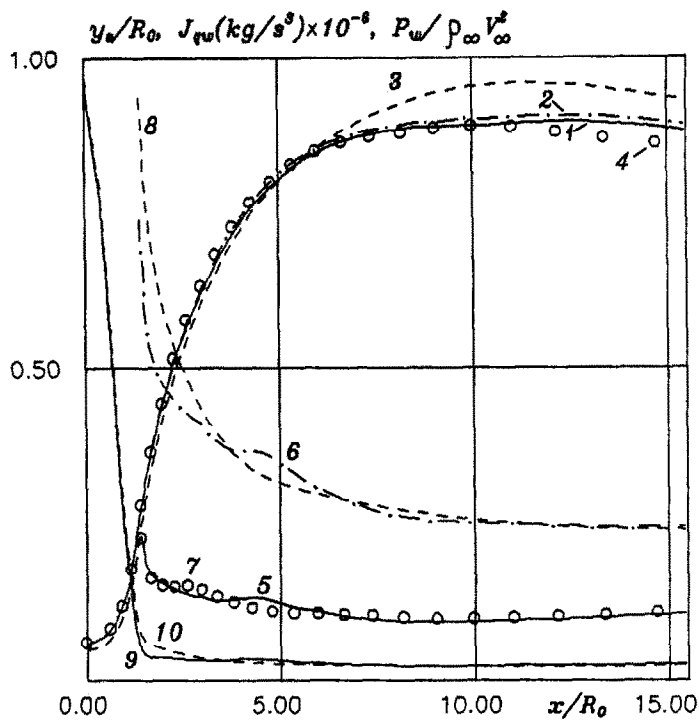
Fig. 1.

Fig. 2.

Figure 2 shows values of the shock detachment distance relative to the nose radius $y'_s = y_s / R_0$ (curves 1–4), the heat flux to the body (curves 5–8), and the dimensionless pressure $P'_w = P_w / \rho_\infty V_\infty^2$ at the body surface (curves 9, 10) along the body (coordinate x') near the bluntness. Curves 1, 5, and 9 (the solid lines) are the results of calculations under thermal

equilibrium and chemical non-equilibrium conditions for a non-catalytic surface and curves 2 and 6 (the dash–dot lines) are those for a fully catalytic surface. From this one can see the maximum effect of the wall catalyticity on the shock detachment distance and the heat flux. The surface catalytic activity has almost no effect on the pressure. The dashed lines 3, 8 and 10 are obtained from calculations under complete (thermal and chemical) equilibrium; the calculations were performed with the previously developed model for calculating chemical equilibrium and chemically frozen flows around slender spherically blunted cones [17]. Curves 4 and 7 (the circles) are the result of a calculation of the shock detachment distance and the heat flux under chemical and thermal non-equilibrium conditions for a non-catalytic surface. with boundary condition (1.17) used for the equation of vibrational relaxation at the surface. (The effect of thermal non-equilibrium on the heat flux to a fully catalytic surface is weak [4].) The corresponding values of the pressure lie precisely on curve 9.

The values of the heat flux at the stagnation point (not shown in Fig. 2) are as follows: for chemically and thermally non-equilibrium flow around a non-catalytic surface $J_{q_w}|_{k_w=0} = 2.78 \times 10^6$ kg/s^3, for chemically non-equilibrium and thermally equilibrium flow $J_{q_w}|_{k_w=\infty} = 2.68 \times 10^6$ kg/s^3, $J_{q_w}|_{k_w=\infty} = 6.24 \times 10^6$ kg/s^3. and for complete equilibrium flow $J_{q_w} = 6.452 \times 10^6$ kg/s^3. We see that the first two values and the last ones are in good agreement with one another.

The closeness of the heat fluxes under thermal equilibrium and non-equilibrium conditions shows that vibrational non-equilibrium is a relatively weak effect in the given flow conditions. The closeness of the heat flux to a fully catalytic surface and the fully equilibrium heat flux at large M_∞ and Re$_\infty$ values confirms that the dissociation model [2] is physically adequate and the numerical implementation of non-equilibrium relaxation-chemical kinetics is correct.

In Fig. 3 the same flow characteristics are shown in the scale condensed in a streamwise direction at greater distances from the stagnation point. Figures 4–8 show the translational and vibrational temperatures across the shock layer at various distances from the stagnation point: the temperature profiles are shown at the stagnation point ($x' = 0$) in Fig. 4, at the conjugation of the spherical and conical surfaces ($x' = 1.4$) in Fig. 5, and at $x' = 7$, 26.9, 60.3 in Figs 6–8.
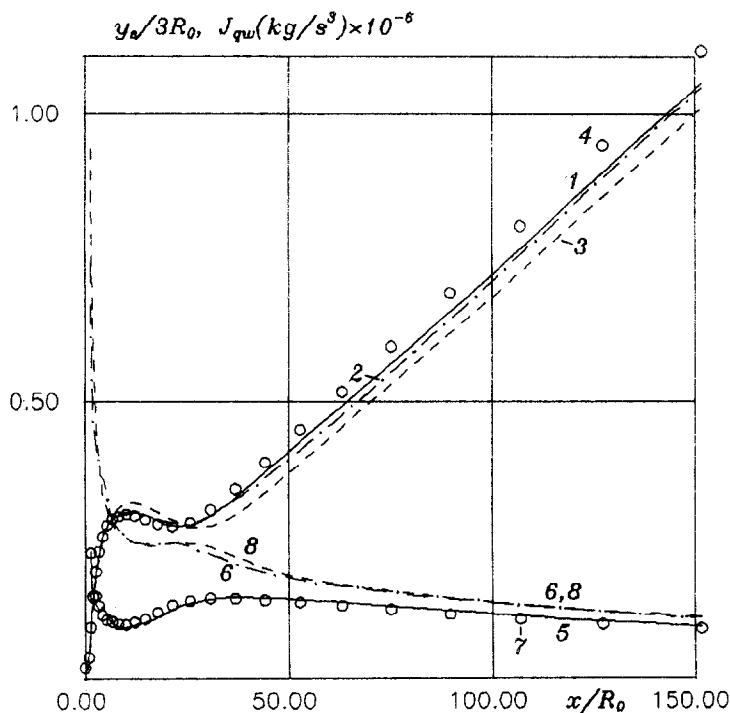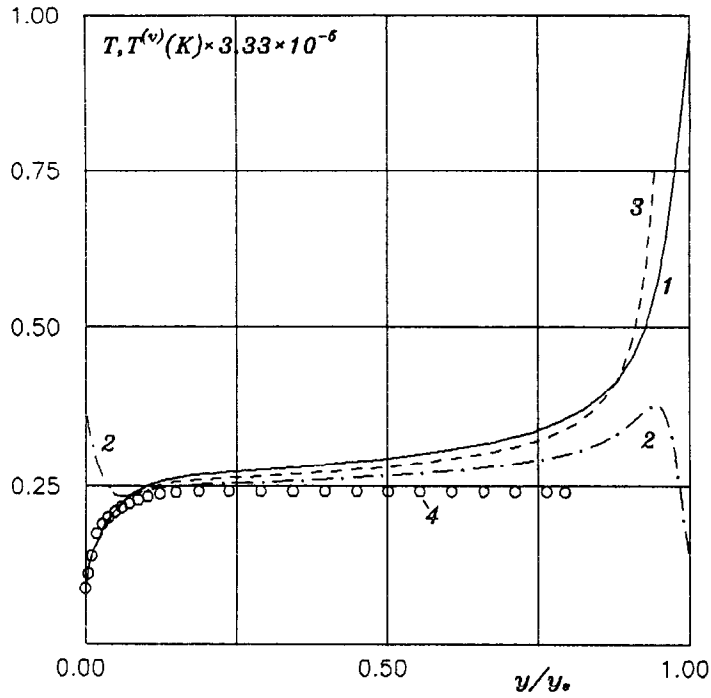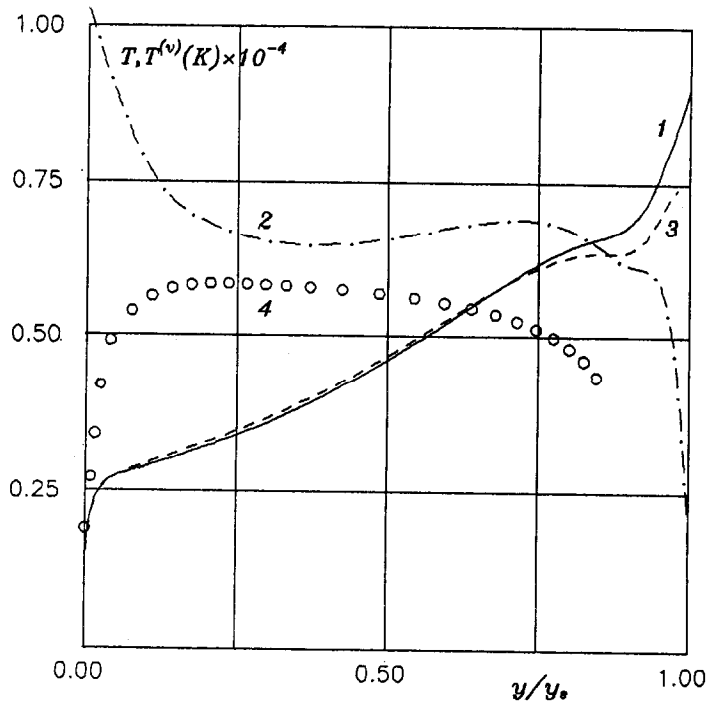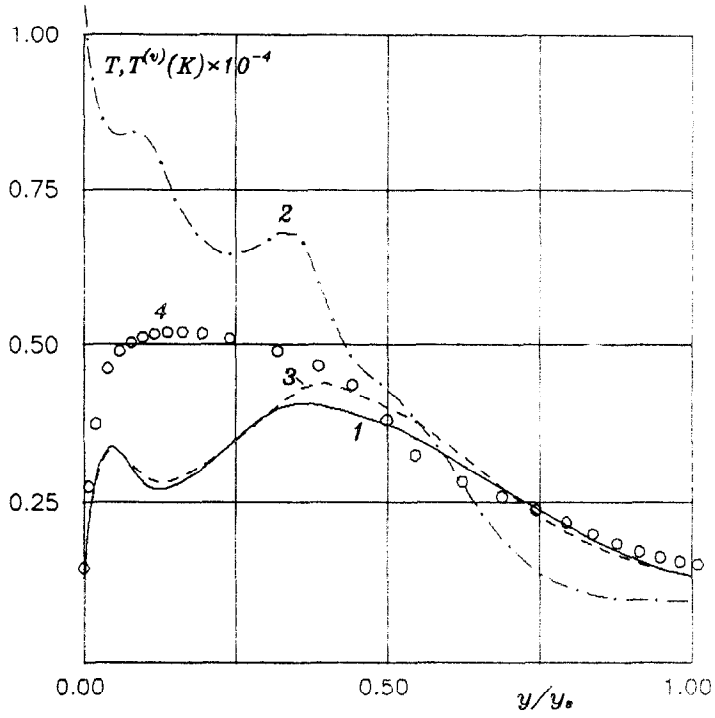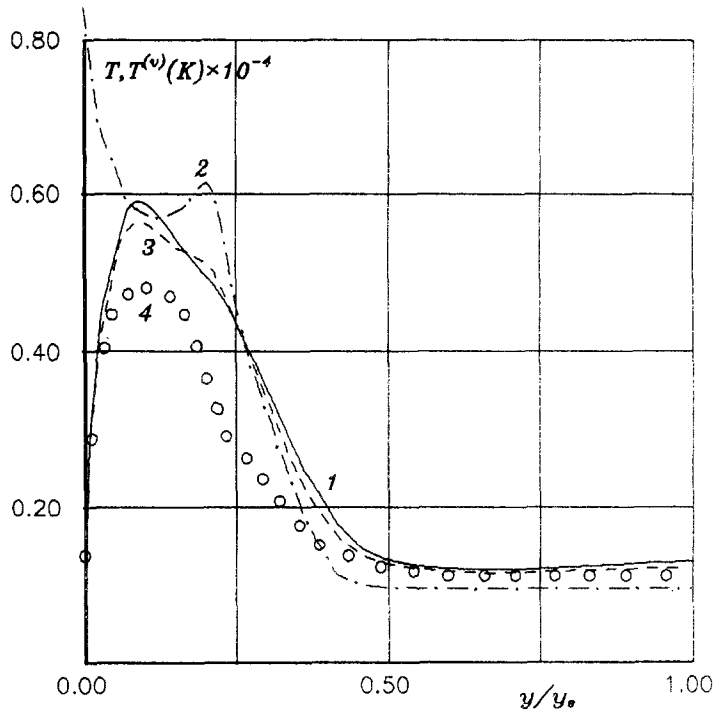

Fig. 3.

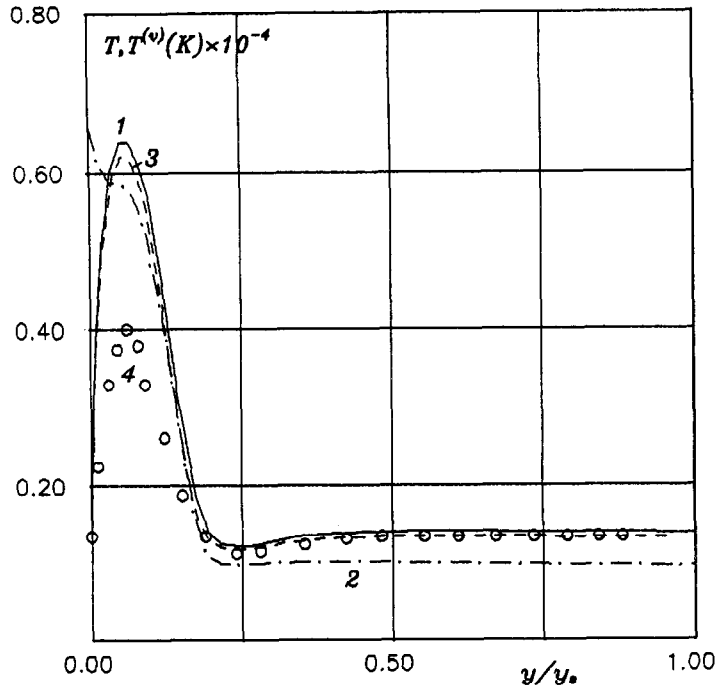Fig. 4.

Fig. 5.

Fig. 6.

Fig. 7.

Fig. 8.

respectively. The body surface is assumed to be non-catalytic. In these figures the solid lines 1 correspond to the translational temperature when there is no thermal equilibrium, the dash–dot lines correspond to the vibrational temperature, dashed lines 3 are obtained from calculations under chemical non-equilibrium and thermal equilibrium conditions, and the circles 4 are the chemical and thermal equilibrium T profiles. In Figs 4–8 the normal coordinate y is related to the chemically and thermally non-equilibrium shock detachment distance.

Analysing Figs 2–8, we find the following physical effects.

1. The closeness of the thermal equilibrium and non-equilibrium flow characteristics in the shock layer over a slender body at high Reynolds and Mach numbers.

2. The closeness of the chemical equilibrium and non-equilibrium values of the pressures on the body, and the closeness of chemical equilibrium and non-equilibrium values of the heat flux, the latter being calculated for a fully catalytic surface.

3. The chemical equilibrium shock detachment distance is greater than the chemical non-equilibrium one at $6 \leqslant x' \leqslant 25$.

This may be explained as follows. In the case of chemical equilibrium,, recombination of nitrogen atoms in the shock layer occurs at a faster rate than in the chemically non-equilibrium case, because of the stronger dependence of the species fractions on the pressure and thermodynamic enthalpy of the expanding chemically equilibrium gas as it moves along the body. Table 1 shows the maximum molar fractions of oxygen and nitrogen atoms across the shock layer at various stations along the body for the fully equilibrium flow and for chemically non-equilibrium thermally equilibrium one. The faster recombination rates under chemical equilibrium lead to more intensive energy production, which raises the temperature in the shock layer. As a result, the gas density falls, and this in turn leads to local thickening of the shock layer. At $x' > 25$ the fully equilibrium shock detachment distance is less than any non-equilibrium one.

4. The strong sensitivity of the non-equilibrium heat flux to changes of the shock detachment distance and pressure along the body.

5. Some difference (to within 4%) between the non-catalytic and fully catalytic values of the shock detachment distance (Fig. 3).

Table 1

$\dfrac{x}{R_0}$	VSL in chemical equilibrium		VSL in chemical non-equilibrium	
	$x_O \times 10^3$	$x_N \times 10^3$	$x_O \times 10^3$	$x_N \times 10^3$
0	235	638	258	649
1.4	269	445	310	578
7.0	292	309	326	521
26.9	322	129	305	322
60.3	339	12.3	314	722

6. The flow in the shock layer becomes qualitatively invariant starting at $x/R_0 \approx 27$ under the free-stream conditions discussed. One can see here a "hot" sublayer near the wall and a "cold" one adjacent to the shock.

7. In the "cold" part of the flow there is no equilibrium between the active and vibrational modes far from the stagnation point.

This is because of the large value of the vibrational time τ_i (see the source term (1.4) in (1.2)) at low temperatures and pressures, i.e. in this part of the layer the flow is both chemically and thermally frozen. However, in the "hot" sublayer the vibrational molecular modes relax quite rapidly with the active ones. The large difference between the translational and vibrational temperatures at the body surface, when zero flux of vibrational energy to the body is assumed, is obviously associated with recombination which supplies a substantial amount of energy to the vibrational quantum states of the molecules near the surface.

We thank S. A. Vasil'yevskii for his comments and interest.

REFERENCES

1. TIRSKII G. A., A theory of hypersonic flow around plane and axisymmetric blunted bodies by a viscous chemically-reacting multicomponent gas with injection present. *Nauchn. Tr. Inst. Mekh. Mosk. Gos. Univ.* **39**, 5–38. 1975.
2. SMEKHOV G. D. and ZHLUKTOV S. V., The dissociation-rate constant for diatomic molecules in the adiabatic model. *Khim. Fiz.* **11**, 9, 1171–1179, 1992.
3. TIRSKII G. A., Thermodynamic non-equilibrium effects for the hypersonic flow of a viscous gas around a body. In: *Models of the Mechanics of Inhomogeneous Systems*, pp. 66–92. Inst. Teor. Prikl. Mekh., Sibir. Otdel. Akad. Nauk SSSR, 1989.
4. ZHLUKTOV S. V. and TIRSKII G. A., The influence of vibrational–dissociational interactions on heat transfer and drag in hypersonic flow past bodies. *Izv. Akad. Nauk SSSR, MZhG.* **3**, 141–151, 1990.
5. MARRONE P. V. and TREANOR C. E., Chemical relaxation with preferential dissociation from excited vibrational levels. *Phys. Fluids* **6**, 9, 1215–1221, 1963.
6. UTYUZHNIKOV S. V., Numerical solution of the full viscous shock layer equations in the problem of hypersonic flow around blunt bodies. In: *Numerical Methods in the Mechanics of a Continuous Medium*. Vych. Tsentr. Sibir. Otdel. Akad. Nauk SSSR **17**, 6, 125–131, 1986.
7. SHCHERBAK V. G., On the influence of multicomponent diffusion and pressure diffusion on element composition in hypersonic flow. *Inzh.-Fiz. Zh.* **59**, 4, 673–674, 1990.
8. TIRSKII G. A., Semiphenomenological derivation of the hydrodynamical equations for a mixture of monatomic gases with excited internal degrees of freedom. In: *Mechanics: Modern Problems*, pp. 79–86, Izd. Mosk. Gos. Univ., 1987.
9. MILLIKAN R. C. and WHITE D. R., Systematics of vibrational relaxation. *J. Chem. Phys.* **39**, 12, 3209–3213, 1963.
10. PARK C., Problems of rate chemistry in the flight regimes of aero-assisted orbital transfer vehicles. AIAA paper No. 84-1730, 1984.
11. PARK C., Assessment of the two-temperature kinetic model for ionizing air. AIAA paper No. 87-1574, 1987.
12. TREANOR C. E. and MARRONE P. V., Effect of dissociation on the rate of vibrational relaxation. *Phys. Fluids* **5**, 9, 1022–1026, 1962.
13. KANG S. W. and DUNN M. G., Hypersonic viscous shock layer with chemical non-equilibrium for spherically blunted cones. *AIAA J.* **10**, 10, 1361–1362, 1972.

14. ANDRIATIS A. V., ZHLUKTOV S. V. and SOKOLOVA I. A., Transport coefficients for an air mixture in chemical non-equilibrium. *Mat. Modelirovaniye* **4**, 1, 44–64, 1992.

15. FERTSIGER J. and KAPER G., T*he Mathematical Theory of Transport Processes in Gases.* Mir, Moscow, 1976.

16. KUZNETSOV V. M. and KUZNETSOV M. M., The boundary conditions for multi-atomic gas flows. *Prikl. Mekh. Tekhn. Fiz.* **4**, 93–102, 1975.

17. VASIL'YEVSKII S. A., TIRSKII G. A. and UTYUZHNIKOV S. V., A numerical method for solving the equations of a viscous shock layer. *Zh. Vych. Mat. Mat. Fiz.* **27**, 5, 741–750, 1987.

18. KOLESNIKOV A. G. and SHCHELIN V. S., Numerical analysis of the accuracy of modelling hypersonic heat exchange in subsonic jets of dissociated nitrogen. *Izv. Akad. Nauk SSSR, MZhG* **2**, 135–143, 1990.

19. ZOBY E. V., LEE K. P., GUPTA R. N., TOMSON R. A. and SIMMONDS A. L., Viscous shock-layer solutions with non-equilibrium chemistry for hypersonic flows past slender bodies. *J. Spacecraft and Rockets* **26**, 4, 221–228, 1989.

Translated by R.L.Z.